

Rationalization and tuning of doublet emission in organic radicals

Claire Tonnelé,^{a,*} David Casanova^{a,b}

^a Donostia International Physics Center (DIPC), 20018 Donostia, Euskadi, Spain

^b Ikerbasque Foundation for Science, 48009 Bilbao, Euskadi, Spain

List of contents

Low-lying electronic states of TTM

Figure S1. Molecular structure of TTM and molecular orbital diagram.

Table S1. Vertical transition energies (in eV) to the lowest excited doublet states, oscillator strength, and dominant contributions computed at the PBE0/6-311G(d,p) level for **1**.

Radical-ligand interactions

Figure S2. Molecular structure of TTM-like model system **0** for $\theta = 90^\circ$ and molecular orbital diagram.

Table S2. Vertical transition energies (in eV) to the lowest excited doublet states, oscillator strength, and dominant contributions computed at the PBE0/6-311G(d,p) level for **0** at $\theta = 90^\circ$.

Figure S3. Evolution of the energy of the SOMO/SUMO (green/purple) and HOMO/LUMO (in grey) of **0** as a function of the dihedral angle θ .

Diabatization of the adiabatic states at the ground state (D_3) geometry of **1**

Table S3. e-/h+ contributions to the relative Mulliken fragment charges of diabatic states Z_{1-4} .

Table S4. Energy (in eV) and transition dipole moment components (in D) of diabatic states Z_{1-4} .

Diabatic Hamiltonian (ground state (D_3) geometry)

Excited state relaxation

Table S5. Bonds and dihedrals at the D_3 and C_2 geometries.

Table S6. Vertical transition energies (in eV) to the lowest excited doublet states, oscillator strength, dominant contributions and transition dipole moment components (in D) computed at the PBE0/6-311G(d,p) level at the C_2 geometry.

Diabatization of the adiabatic states computed at the D_1 optimized geometry of **1**

Table S7. e-/h+ contributions to the relative Mulliken fragment charges of diabatic states Z_{1-4} .

Figure S4. TTM molecule with vector representation of TDMs of Z_{1-4} diabatic states at the lowest excited state (C_2) geometry of **1**.

Table S8. Energy (in eV) and transition dipole moment components (in D) of diabatic states Z_{1-4} at the lowest excited state (C_2) geometry of **1**.

Substituted TTM

Figure S5. Energy of the SOMO/SUMO (green/purple) and HOMO/LUMO (in grey) for **1**, **1H**, **1NO₂**, **1NH₂**, **1'NH₂**, and **1''NH₂**.

Table S9. Vertical transition energies (in eV) to the lowest excited doublet state, oscillator strength, and dominant contributions computed at the PBE0/6-311G(d,p) level for **1H**, **1NO₂**, **1NH₂**, **1'NH₂**, and **1''NH₂**.

Low-lying electronic states of TTM

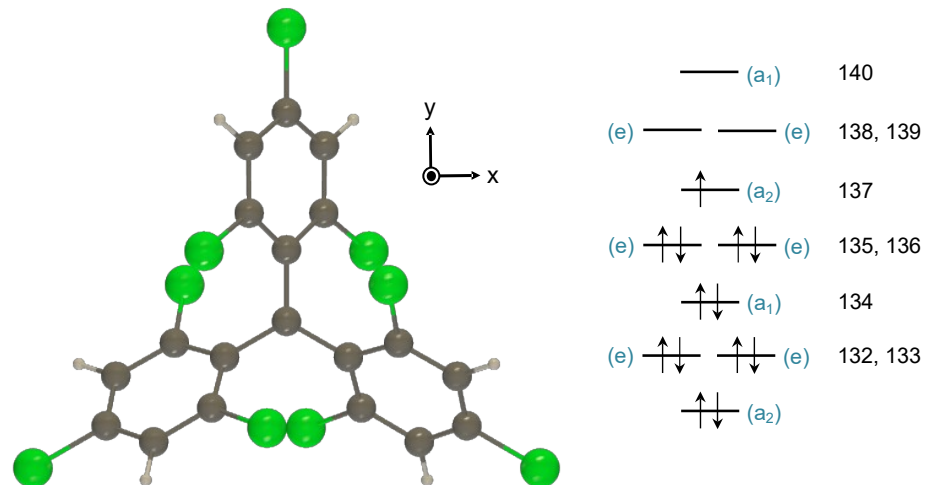


Figure S1. Molecular structure of TTM and molecular orbital diagram.

Table S1. Vertical transition energies (in eV) to the lowest excited doublet states, oscillator strength, and dominant contributions computed at the PBE0/6-311G(d,p) level for **1**.

state	E	f	contrib.	coeff
1 (E)	2.904	0.027	137A<138A	0.284
			133B<137B	-0.264
			136B<137B	0.885
2 (E)	2.904	0.027	137A<139A	-0.284
			132B<137B	0.264
			135B<137B	0.885
3 (E)	3.173	0.004	137A<138A	-0.225
			133B<137B	0.878
			136B<137B	0.348
4 (E)	3.173	0.004	137A<139A	-0.225
			132B<137B	0.878
			135B<137B	-0.348
5 (A₁)	3.195	0.009	137A<140A	0.209
			134B<137B	0.957
6 (A₂)	3.324	0	137A<146A	-0.252
			131B<137B	0.883
7 (E)	3.598	0.222	137A<139A	0.830
			132B<137B	0.329
			135B<137B	0.240
8 (E)	3.598	0.222	137A<138A	0.830
			133B<137B	0.329
			136B<137B	-0.240

reported contributions ≥ 0.2 only

Radical-ligand interactions

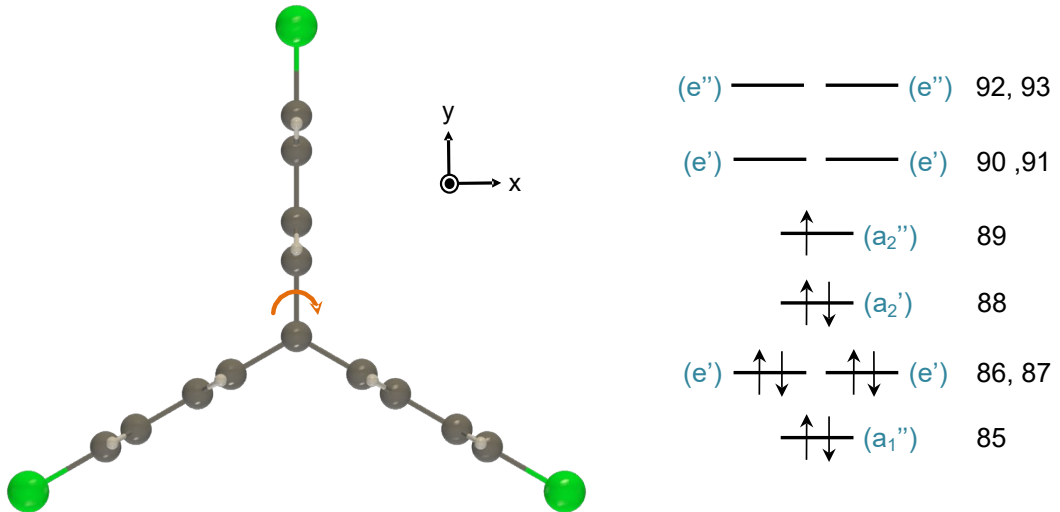


Figure S2. Molecular structure of TTM-like model system **0** for $\theta = 90^\circ$ and molecular orbital diagram.

Table S2. Vertical transition energies (in eV) to the lowest excited doublet states, oscillator strength, and dominant contributions computed at the PBE0/6-311G(d,p) level for **0** at $\theta = 90^\circ$.

state	E	f	contributions	coeff
1 (A_1'')	3.820	0	88B < 89B	0.99044
5 (E'')	4.182	0	86B < 89B	0.97606
6 (E'')	4.182	0	87B < 89B	0.97606
7 (E'')	4.285	0	89A < 91A	0.99235
8 (E'')	4.285	0	89A < 90A	0.99235

reported contributions ≥ 0.2 only

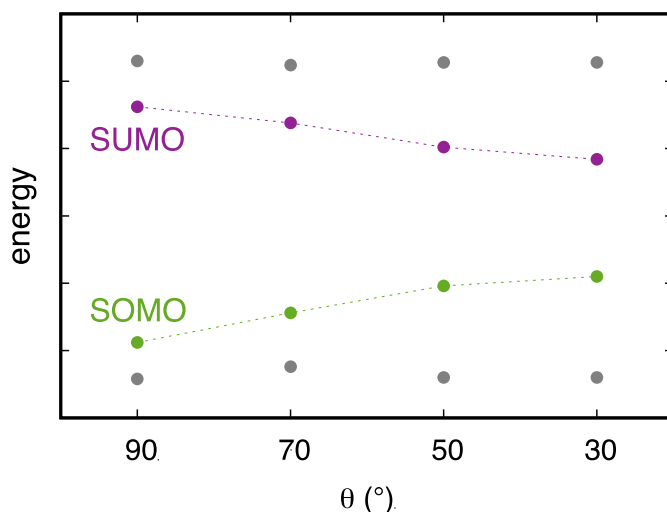


Figure S3. Evolution of the energy of the SOMO/SUMO (green/purple) and HOMO/LUMO (in grey) of **0** as a function of the dihedral angle θ .

Diabatization of the adiabatic states at the ground state (D_3) geometry of 1

Table S3. e-/h+ contributions to the relative Mulliken fragment charges of diabatic states Z_{1-4} .

state	Z_1 (LC_x)		Z_2 (LC_y)		Z_3 (CL_y)		Z_4 (CL_x)	
	β h+	β e-	β h+	β e-	α h+	α e-	α h+	α e-
central C	0.011	-0.442	0.011	-0.442	0.262	-0.024	0.262	-0.024
ligand (1)	0.322	-0.178	0.322	-0.178	0.194	-0.274	0.194	-0.274
ligand (2)	0.122	-0.173	0.522	-0.184	0.258	-0.477	0.131	-0.070
ligand (3)	0.522	-0.184	0.122	-0.173	0.131	-0.070	0.258	-0.477

Table S4. Energy (in eV) and transition dipole moment components (in D) of diabatic states Z_{1-4} .

	E	TDM(x)	TDM(y)	TDM(z)
Z_1 (LC_x)	3.043	2.258	-2.258	0.000
Z_2 (LC_y)	3.043	-2.258	-2.258	0.000
Z_3 (CL_y)	3.458	2.057	2.057	0.000
Z_4 (CL_x)	3.458	-2.057	2.057	0.000

Diabatic Hamiltonian (ground state (D_3) geometry)

diabatic H	Z1	Z2	Z3	Z4
Z1	3.043	0.000	0.000	-0.278
Z2	0.000	3.043	-0.278	0.000
Z3	0.000	-0.278	3.458	0.000
Z4	-0.278	0.000	0.000	3.458

Excited state relaxation

Table S5. Bonds and dihedrals at the D_3 and C_2 geometries.

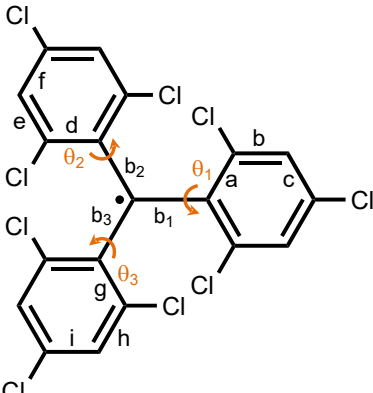
	D_3 geometry	C_2 geometry
		
θ_1	49.7	45.1
θ_2	49.7	44.3
θ_3	49.7	43.8
b_1	1.470	1.428
b_2	1.470	1.454
b_3	1.470	1.454
a	1.407	1.458
d / g	1.407	1.414
b	1.382	1.364
e / h	1.382	1.379
c	1.382	1.399
f / i	1.382	1.386

Table S6. Vertical transition energies (in eV) to the lowest excited doublet states, oscillator strength, dominant contributions and transition dipole moment components (in D) computed at the PBE0/6-311G(d,p) level at the C_2 geometry.

state	E	f	contributions	coeff	TDM(x)	TDM(y)	TDM(z)
D_1 (E)	2.421	0.035	137A < 138A 136B < 137B	-0.300 0.930	0	-0.769	0
D_2 (E)	2.673	0.034	137A < 139A 135B < 137B	-0.262 0.936	0.723	0	-0.044
D_7 (E)	3.319	0.273	137A < 138A 133B < 137B 136B < 137B	0.816 0.366 0.279	0	-1.833	0
D_8 (E)	3.480	0.251	137A < 139A 132B < 137B 135B < 137B	0.854 -0.274 0.271	1.715	0	0.002

Diabatization of the adiabatic states at the lowest excited state (C_2) geometry of 1

Table S7. e-/h+ contributions to the relative Mulliken fragment charges of diabatic states Z_{1-4} .

state	Z_1		Z_2		Z_3		Z_4	
	$\beta h+$	$\beta e-$	$\beta h+$	$\beta e-$	$\alpha h+$	$\alpha e-$	$\alpha h+$	$\alpha e-$
central C	0.018	-0.377	0.009	-0.374	0.215	-0.019	0.242	-0.019
ligand (1)	0.641	-0.229	0.108	-0.229	0.301	-0.504	0.174	-0.029
ligand (2)	0.156	-0.183	0.431	-0.189	0.140	-0.136	0.221	-0.405
ligand (3)	0.156	-0.183	0.431	-0.189	0.140	-0.136	0.221	-0.405

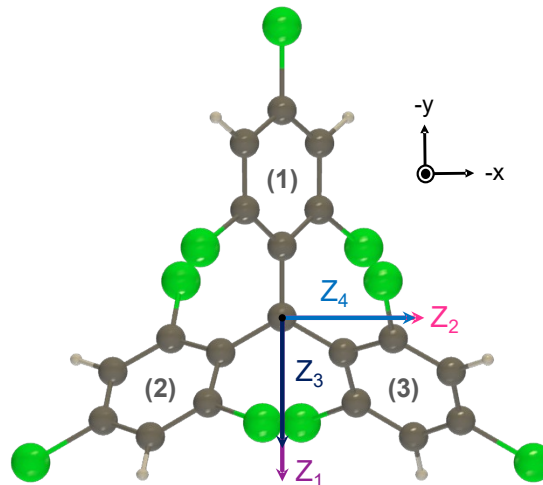


Figure S4. TTM molecule with vector representation of TDMs of Z_{1-4} diabatic states at the lowest excited state (C_2) geometry of 1.

Table S8. Energy (in eV) and transition dipole moment components (in D) of diabatic states Z_{1-4} at the lowest excited state (C_2) geometry of 1.

	E	TDM(x)	TDM(y)	TDM(z)
Z_1	2.421	0.000	3.968	0.000
Z_2	2.673	-3.451	0.000	0.100
Z_3	3.108	0.000	3.126	0.000
Z_4	3.347	-3.236	0.000	-0.050

Diabatic Hamiltonian (C_2 geometry)

diabatic H	Z1	Z2	Z3	Z4
Z1	2.632	0.000	0.381	0.000
Z2	0.000	2.807	0.000	0.300
Z3	0.381	0.000	3.108	0.000
Z4	0.000	0.300	0.000	3.347

Substituted TTM

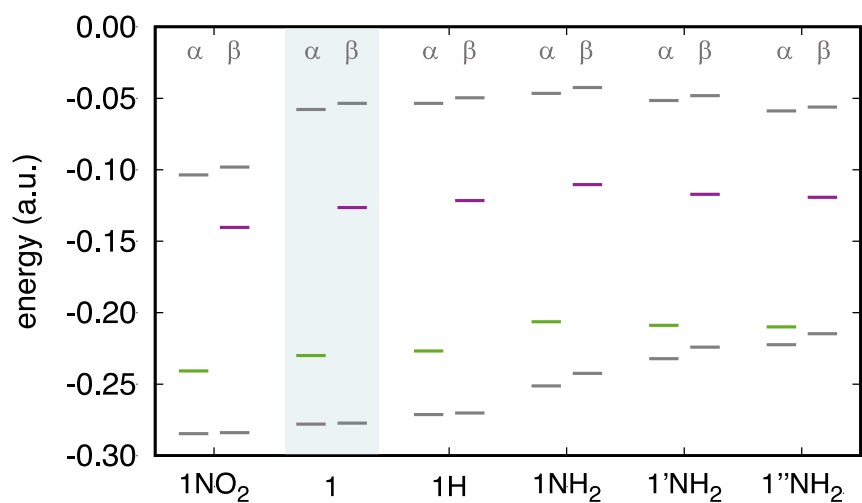


Figure S5. Energy of the SOMO/SUMO (green/purple) and HOMO/LUMO (in grey) for **1**, **1H**, **1NO₂**, **1NH₂**, **1'NH₂**, and **1''NH₂**.

Table S9. Vertical transition energies (in eV) to the lowest excited doublet state, oscillator strength, and dominant contributions (coefficient ≥ 0.2) computed at the PBE0/6-311G(d,p) level for **1H**, **1NO₂**, **1NH₂**, **1'NH₂**, and **1''NH₂**.

molecule	E	f	contrib.	coeff
1H	2.906	0.018	SOMO<LUMO	0.255
			HOMO-2<SUMO	0.492
			HOMO<SUMO	0.781
1NO₂	2.764	0.018	SOMO<LUMO	0.730
			HOMO-5<SUMO	0.268
			HOMO-4<SUMO	-0.364
1NH₂	2.548	0.082	HOMO-1<SUMO	-0.420
			HOMO<SUMO	0.954
			HOMO-2<SUMO	0.943
1'NH₂	2.243	0.133	HOMO-1<SUMO	0.221
			HOMO<SUMO	0.958
1''NH₂	2.158	0.119	HOMO-1<SUMO	0.221
			HOMO<SUMO	0.958